JOURNAL OF APPLIED POLYMER SCIENCE VOL. 19, PP. 303–317 (1975)

Studies on the Biaxial Stretching of Polypropylene Film. XI. Type II Orientation During [2-2FI]-Type Stretching and its Change by Subsequent Thermal Contraction

NOBORU IWATO, HIROSHI TANAKA,* and SABURO OKAJIMA,*
Faculty of Technology, Tokyo Metropolitan University, Setagaya-ku, Tokyo, Japan

Synopsis

In order to study the deformation mechanism of type II stretching, the change in orientation during the restretching and subsequent thermal contraction was investigated by x-ray diffraction method. When a uniaxially oriented film is restretched, the lamellae which are stacked in the stretching direction by the stretching rotate as a whole toward the restretching axis. They rotate backward nearly reversibly during the thermal contraction, unless the restretching exceeds a balancing state, where the orientation in the film plane are equal in all directions. However, when the restretching degree is so high and the film orientation exceeds the balancing state, the lamellar rotation is accompanied by a complex phenomenon. It is considered from the wide-angle and small-angle x-ray diffraction patterns that the lamellar surface becomes indented because of slippage between microfibrils composing the lamellae, and the microfibrils themselves bend at the boundary between the amorphous and crystalline regions within which the tilting of *c*-axis also occurs. Upon contracting of the film; these changes recover, but even in the last stage of contraction the orientation approaches the symmetrical biaxial orientation but not the uniaxial orientation from which the biaxial orientation is started. These orientation and disorientation behaviors are not affected basically by a slight change in the restretching temperature and the degree of stretching.

INTRODUCTION

The fine structure of a film biaxially stretched to a balanced state is conspicuously dependent on the type of biaxial stretching as reported previously.[1] Although this is not only interesting from a theoretical viewpoint of deformation mechanism of crystalline polymer, but it is also important with regard to a practical problem such as shrinkable film,[2] and few authors have studied this problem. The orientation mechanisms of type I[3–7] and type III[1,8] were reported in the previous papers; hence, the orientation during type II[1] stretching and its change due to subsequent thermal contraction are the subject of the present paper. It has been described[1] that [2-2FI]-type stretching, namely, stretching of a film with width unrestrained at temperature T_1 followed by restretching at temperature T_2 perpendicularly to the stretching direction with insertion of a cooling pro-

* Present address: Faculty of Engineering, Yamagata University, Yonezawa, Japan.

cess to room temperature between the stretching and the restretching gives rise to type II orientation unless T_2 is 15–20°C higher than T_1; and that especially when polypropylene film quenched to −20°C is stretched at 130°C ($T_1 = T_2$), a simple relation holds for L_p, θ_w and θ_s,

$$L_p = L_0 \cos (\theta_w - \theta_s) \quad (1)$$

where L_p is the diagonal long period of the restretched film, L_0 is the long period before restretching, and θ_w and θ_s are the rotation angles of c-axis and lamella, respectively. Therefore, this simplest case is omitted from the following description.

EXPERIMENTAL

Sample Film. Sample film B_6 was mainly used besides B_3, whose characteristics are listed in Table I. The samples were melt pressed at 210°C for 5 min and quenched in ice water to films 150–250 μ thick.

Biaxial Stretching. [2-2FI]-Type stretching was carried out in polyethylene glycol with width unrestrained, the condition of which was indicated with the symbols defined previously.[1] The degrees of stretching (v_1) and restretching (v_2) were expressed in relation to the respective dimensions immediately before preheatings for stretching and restretching, respectively. Both rates of stretching and restretching were 100%/min. The maximum value of v_1 was 3.5–4 because when v_1 was larger than 3.5–4, restretching could not be carried out owing to too easy splitting of the film.

Thermal Contraction. Specimens, 3 × 5 cm, were cut from a biaxially stretched film, and each specimen was heated in air at a desired temperature between 120° and 170°C for 15 min, and the dimensions l_{pp} and l_{ps} along the stretching direction (pp) and the restretching direction (ps), respectively, were measured as a function of temperature.

X-Ray Diffraction Photograph. X-Ray diffraction photographs were taken with Ni-filtered CuK_α radiation at 35 kV × 15 mA for wide-angle x-ray diffraction (WAXD) study and at 45 kV × 100 mA for small-angle x-ray scattering (SAXS) study. For this purpose, an x-ray diffractometer, Rotaflex RU-3V of Rigaku Denki Co., Ltd., was used. All the samples in this study showed the diffraction patterns of monoclinic crystal after preheating.

Small-Angle Light Scattering (SALS). Small-angle light-scattering model texture was prepared by photographing hand-drawn pattern to scale

TABLE I
Characteristics of Isotactic Polypropylene Sample

Sample	Molecular weight $\bar{M}_v$[a]	Tacticity,[b] %
B_3	36.4×10^4	96
B_6	28.9×10^4	96

[a] Evaluated by equation of Kinsinger and Hughes.[11]
[b] Extracted with boiling n-heptane.

7:100 by taking into consideration the wavelength of laser (6328 Å) used as a light source for the SALS study.

RESULTS AND DISCUSSION

The orientation and disorientation behavior of a film during restretching and thermal contraction, respectively, seems to depend on the degree of restretching besides the film character. Hence, the study was divided into two ranges: in A, contraction was performed from a state of balanced orientation, while in B, behavior of the overstretched film was examined. The contraction behavior differs considerably between A and B as mentioned below.

Range A

[2-2FI](130)$_p\langle 3.5 \times v_2\rangle$ stretching was carried out on B_6. It is seen from Figure 1 that the orientation in this case is typically of type II, and a nearly balanced orientation is brought about by the restretching 2.0× (Fig. 1c), where the orientation axes are at angles ±45° with *ps*. We denote hereafter this type of orientation as symmetric biaxial orientation. However, when the film is restretched beyond the balanced orientation, an additional small intensity maximum appears at the meridian of each diffraction ring, as shown by a six-point diagram (Figs. 1d and 1e). In such a case, three orientation axes seem to exist, among which the two off-meridional axes are the rotating axes, inclination of which to *ps* decreases with

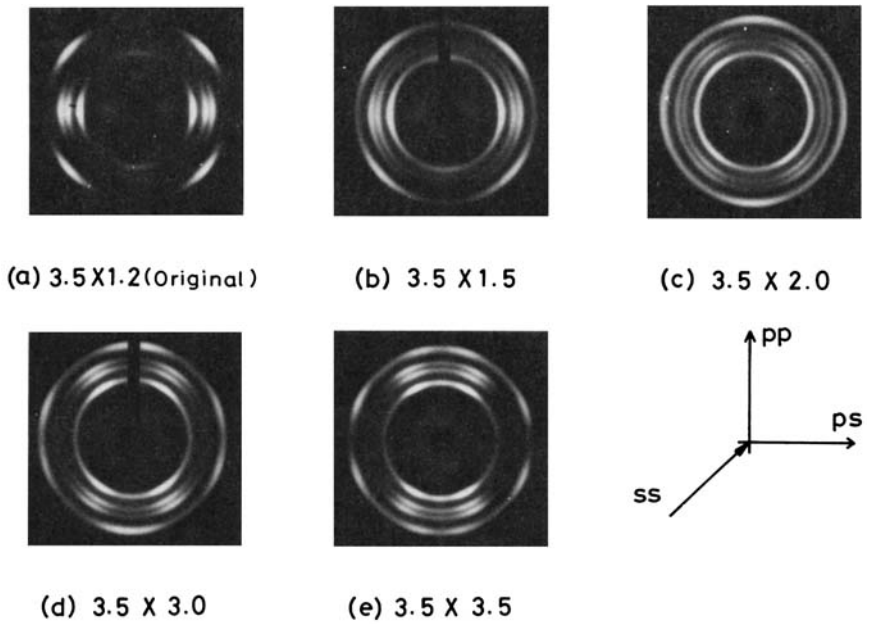

Fig. 1. Change of WAXD pattern during restretching [2–2FI](130)$_p\langle 3.5 \times v_2\rangle$.

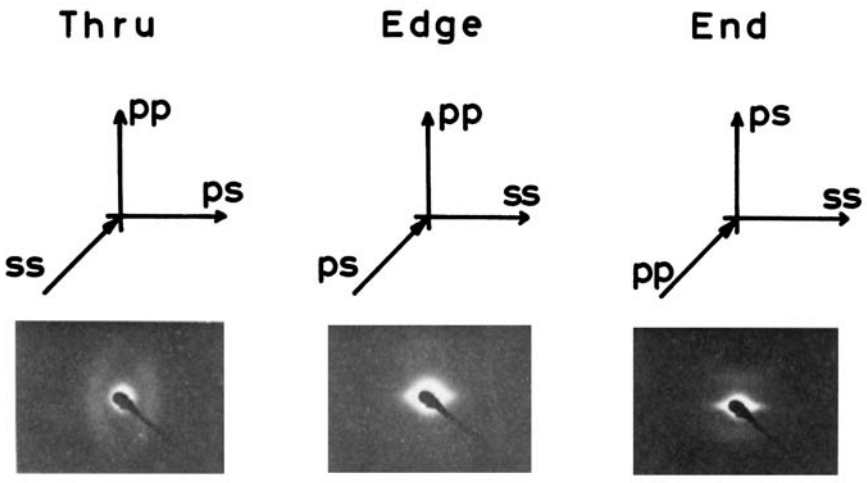

Fig. 2. SAXS pattern of a specimen prepared by stretching [2–2FI](130)$_p$⟨2.8 × 4.1⟩.

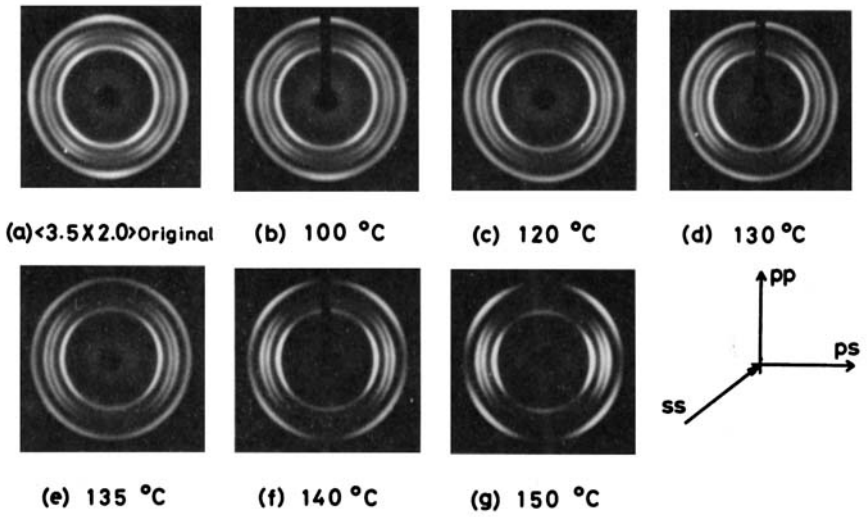

Fig. 3. Change in WAXD pattern of film prepared by stretching [2–2FI](130)$_p$⟨3.5 × 2.0⟩ during thermal contraction at 100–150°C.

v_2. Corresponding to the meridional maximum intensity, stacking of a small fraction of lamellae in the direction *ps* is evidenced by the SAXS pattern. Figure 2 is an example produced by a [2-2FI](130)$_p$⟨2.8 × 4.1⟩ stretching, in which a line pattern appears in the end view but not in the edge view.

Another type of six-point pattern is also seen in Figure 1c, where an intensity maximum can be seen very faintly at the equator of each diffraction ring instead of at the meridian (it is more clearly observed on the negative film and ascertained by recording). Therefore, a small fraction of lamellar crystal persistently remains unrotated at such a small value of v_2.

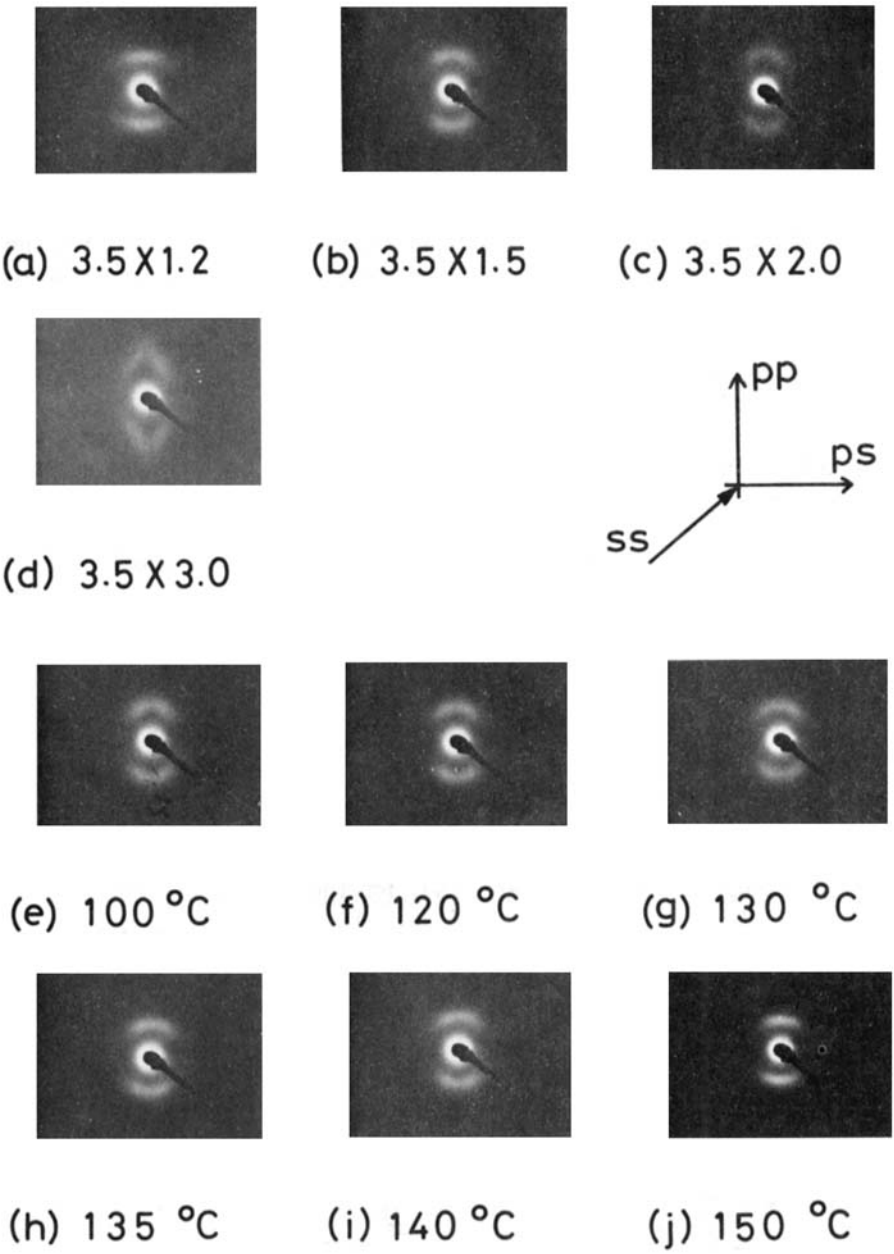

Fig. 4. SAXS patterns corresponding to WAXD patterns in Figs. 1 and 3.

When the film shown in Figure 1c is thermally contracted from a balanced orientation, both WAXD and SAXS patterns return nearly reversibly toward those before restretching as shown in Figures 3 and 4, respectively.

An example of reversible change of film dimension during stretching and restretching at 130°C and subsequent thermal contraction was already

reported (ref. 2, Fig. 1). This corresponds to the x-ray investigation mentioned here.

The long period is slightly but clearly larger in Figures 4i and 4j compared with the other diagrams in Figure 4. This may be a result of annealing during the thermal contraction at higher temperature, which has never been experienced by the film.

A similar result is also obtained in the restretching of [2-2FI](130)$_p$⟨2.7 × v_2⟩ and [2-2FI](152)$_p$⟨2.7 × v_2⟩. Therefore, it may be concluded that the lamellar crystals rotated in the course of restretching return nearly reversibly to the original orientation during the subsequent thermal contraction unless the restretching exceeds the balanced state, and this is basically not affected by differences in temperature of deformation between 130° and 152°C as well as v_1. These phenomena are apparently very simple in this case; and the deformation and contraction mechanisms are easily envisioned, in contrast to that described in the next section, except for the behavior of a small fraction of matter exhibiting the maximum intensity of diffraction at the equator or meridian of the six-point diagram. Although the diffraction is unusual, it is attributable to the behavior of only a small fraction of matter which may barely affect the principal trend of orientation or disorientation.

Range B

B_6, [2-2FI](152)$_p$⟨3.5 × v_2⟩

The dimensional change of a square film specimen during stretching, restretching, and subsequent thermal contraction is shown in Figure 5. A(1.82) indicates the dimension after stretching 3.5×, which contracts to B during the preheating at 152°C for the subsequent restretching.

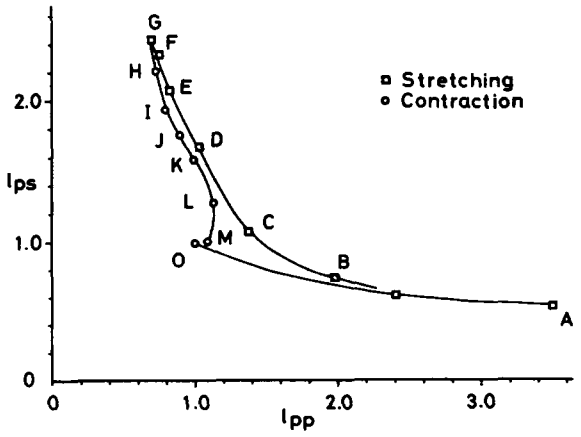

Fig. 5. Dimensional change in film during biaxial stretching and subsequent thermal contraction. T_1 = T_2 = 152°C. Contraction temperature, °C: H(120), I(140), J(150), K(155), L(160), M(170).

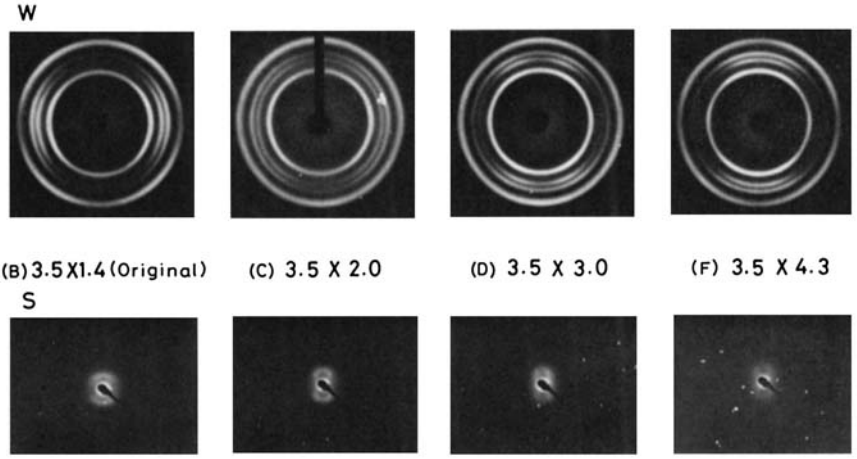

Fig. 6. Changes in WAXD and SAXS patterns during restretching at 152°C.

Upon restretching the film B to 4.4×, the dimension changes from B(1.30) to G(1.71) through C(1.48), D(1.71), E(1.70), and F(1.71). It is seen from the change in the numbers in the brackets, indicating $l_{pp} \times l_{ps}$, that the film area is kept constant during the restretching from D to G. When film G is heated, it contracts from G to M(1.08) through H(1.61), I(1.55), J(1.57), K(1.55), and L(1.45) as the temperature rises, where $l_{pp} \times l_{ps}$ is unchanged to 155°C and then drops steeply. It is interesting that $\overrightarrow{DG}$ and $\overrightarrow{GK}$ are parallel to each other within the ranges of constant area and the critical temperature 150–155°C nearly coincides with the restretching temperature. This implies that restretching and contraction occur nearly two-dimensionally when the film has the overbalanced orientation, and the two-dimensional contraction converts into three-dimensional one when the temperature exceeds T_2, the highest temperature experienced by the film.

This behavior of two-dimensional change of the film area restretched at 152°C closely resembles the result obtained on the film restretched at 130°C,[2] and is in good agreement with the fact that the refractive index along thickness direction n_{ss} is kept constant during the restretching and contraction as already reported in part I of this series of studies.[9]

WAXD (Figs. 6W and 7W) and SAXS (Figs. 6S and 7S) exhibit forward and backward rotation of lamellar crystals during restretching and contraction, respectively (Fig. 5). It is noticed that a six-point pattern is also observed in Figure 6W; however, it is very faint compared with the pattern in the case of the 130°C stretching.

The SAXS pattern of the overrestretched film 6F is of a type which has barely been reported. It may be considered that the pattern shows an extremely broad distribution of lamellar orientation angle and that a small fraction of lamellae stacking in the *ps* direction is contained there.

As to the film contraction from G, the disorientation behavior is not completely reversible and differs from that described in range A. The

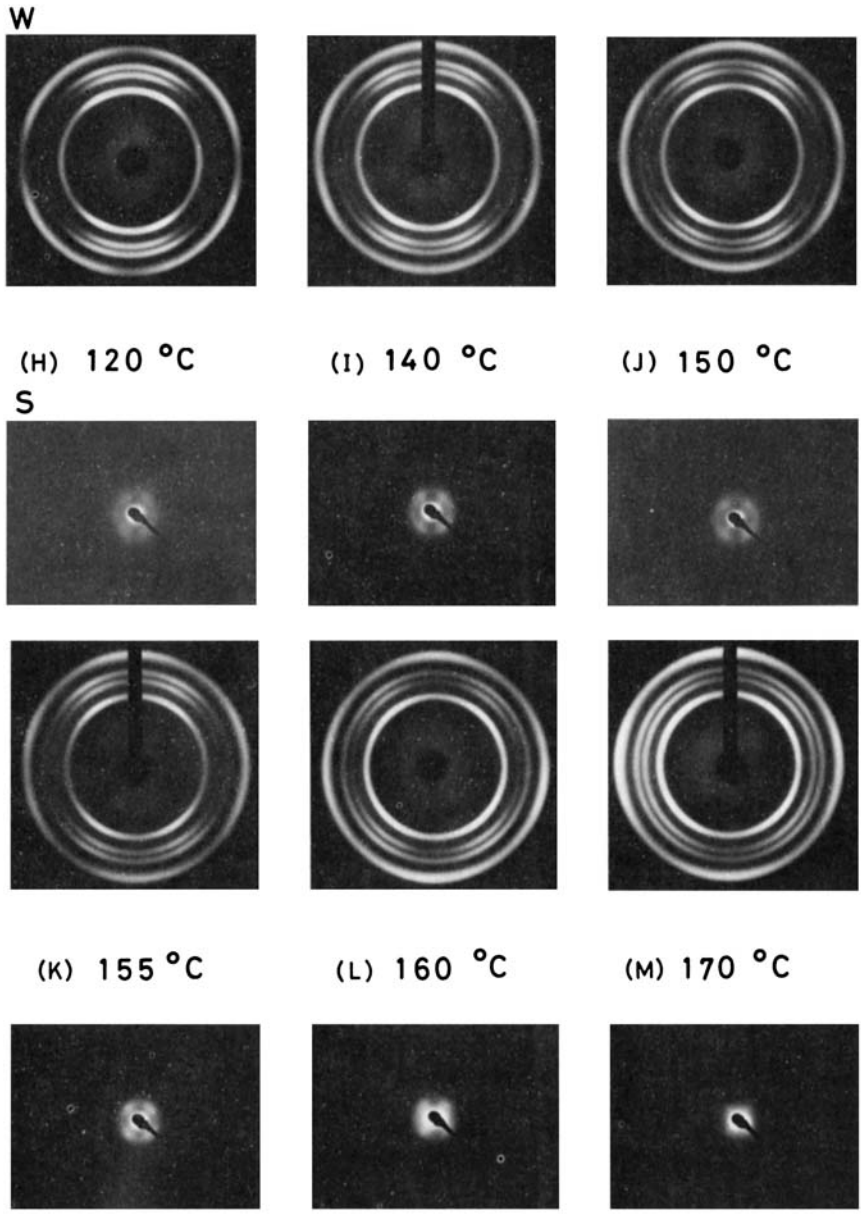

Fig. 7. Changes in WAXD and SAXS patterns during thermal contraction.

contracted film always shows a four-point diagram, at least within the range of the experimental temperature, which approaches gradually that of the symmetric biaxial orientation in the order from G to M, but not to the two-point diagram as indicated by B or C (uniaxial orientation). The above phenomenon corresponds to the following: $\overrightarrow{GM}$ in Figure 5 runs almost parallel to $\overrightarrow{GC}$, but does not so steadily follow the line to $\overrightarrow{CB}$, as shown in

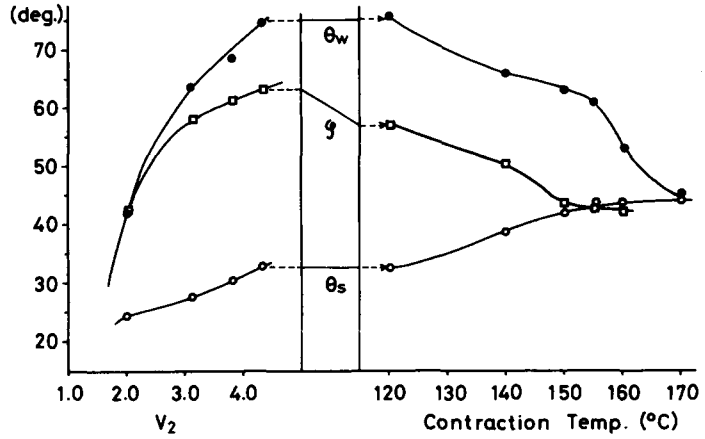

Fig. 8. Change in orientation parameters during restretching at 152°C and thermal contraction. θ_w: orientation angle of c-axis; φ: orientation angle of lamellar stacking axis; θ_s: rotation angle of lamellar crystal.

the contraction curve of a film restretched beneath the balancing point (Fig. 1 in ref. 2).

The symmetric biaxial orientation is a type of isotropic texture but differs completely from that of the original unstretched film, which is spherulitic and has random orientation of lamellar crystals. Of course, when the contraction temperature is further raised, the random orientation may appear, a symptom of which is already presented by the arc broadening in Figures 7K and 7L. The $l_{pp} \times l_{ps}$ of 7L is already 1.08; nevertheless, the biaxial orientation axes are still crossing nearly perpendicularly. It is interesting that a symmetric biaxial orientation can be observed as a considerably stable isotropic texture.

It is clearly seen that the last two films have somewhat increased long periods. We will return later again to this point.

For the purpose of a more or less quantitative study of the phenomenon, θ_w, θ_s, and φ are plotted in Figure 8 against v_2 and the contraction temperature, providing the overall orientation can be represented by the parameter read at the point of maximum intensity on the diffraction arc. Here, θ_w is the orientation angle of the c-axis, θ_s is the angle of rotation of lamellar crystals, and φ is the angle between the stacking direction K of lamellar crystals and pp. Figure 9 is a schematic illustration of these parameters, where the left-hand photographs are the model textures and the corresponding SALS pattern is shown at the right side of each model. The textures (a)–(c) are composed of lamellae with smooth surfaces, while the texture (d) is composed of lamellae with indented surfaces whose SALS is less sharp in comparison with those of the (a)–(c) textures; (e) shows the case in which lamellae with $\theta_s = \varphi = 90°$ are contained among those with $\theta_s = 35°$ and $\varphi = 65°$. The corresponding SALS pattern supposedly is more similar to Figure 6F when the lamellae are distributed more or less around the positions shown in the model texture.

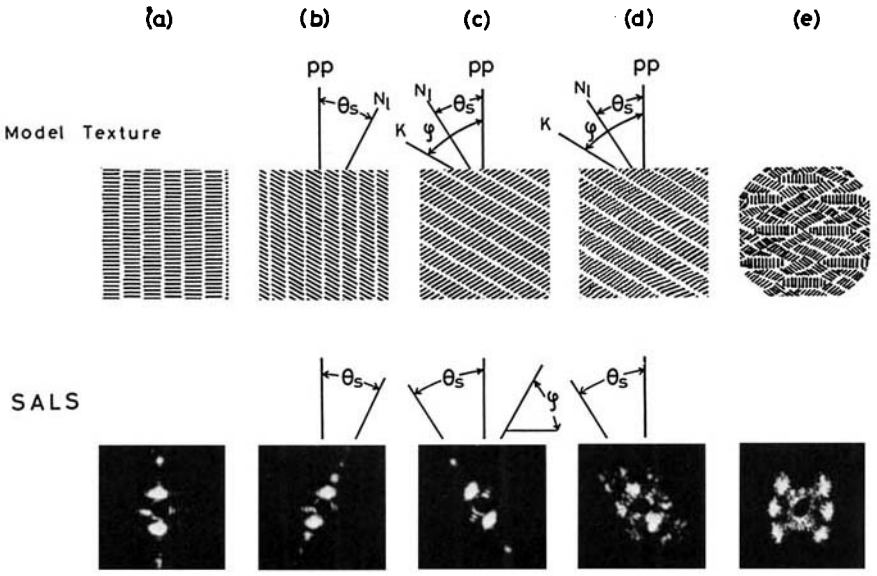

Fig. 9. Schematic illustration of θ_w, φ, and θ_s. Left-hand photographs: model textures; right-hand photographs: SALS from each model texture.

These parameters could definitely be determined. However, in the case of a restretched film at 130°C, especially for v_2 larger than 3, the determination was ill-defined because of the broadening of the diffraction arc, although it was improved considerably after thermal contraction.

The parameters change during restretching and subsequent thermal contraction, as Figure 8 shows; θ_w and φ steeply increase with restretching and amount to 45° already at $v_2 = 2$; φ is slightly smaller than θ_w but much larger than θ_s. From this fact it is supposed that the microfibril is bending at the boundary between the crystalline and amorphous parts by tilting (Fig. 10e), and this bending increases with v_2. A large difference between θ_w and θ_s may be caused by the tilting as well as indention of the lamellar surface due to slipping between microfibrils (Figs. 10d and 10e).

When film G is contracted, θ_w and φ decrease while θ_s increases further and both φ and θ_s amount to 45° at 150°C which almost coincides with the temperature of stretching and restretching (Fig. 8). Upon elevating further the contraction temperature, θ_w drops steeply to 45° at 170°C, while θ_s and φ remain unchanged. Therefore, all the three parameters take the value of 45° in the final stage of contraction. This phenomenon means that the contracted film approaches symmetric biaxial orientation.

In order to illustrate the change of fine structure during type III orientation, we have proposed a model[8] which is simplified and idealized but sufficient for explanation of the principle. According to this model, stretched film is principally composed of bundles of microfibrils (mf) aligned along *pp*, and the crystalline region (folded type) within each microfibril merges laterally to lamellar crystal by fitting nearly crystallo-

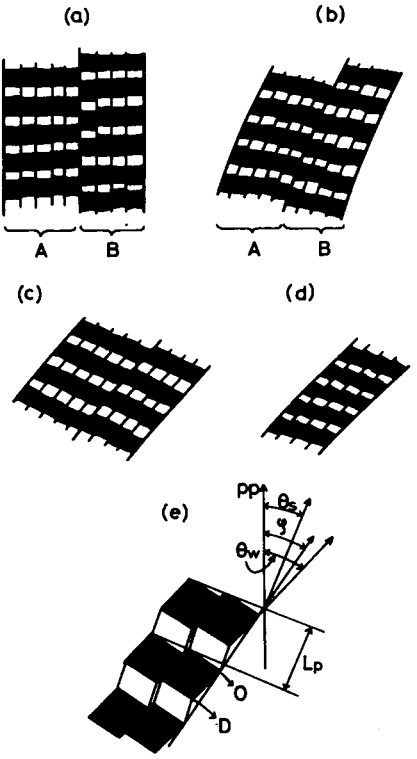

Fig. 10. Schematic illustration of change in fine structure during restretching.

graphically on the lateral surfaces of neighboring microfibrils[10] (Fig. 10a). The structure is not uniform but there are irregularities of different orders: (1) within microfibril itself, (2) between microfibrils, and (3) between blocks of microfibrils. These irregularities as well as thermal distortion play a role in the deformation of various types. The model is also useful for the present study but with a slight modification.

Upon restretching ($v_2 < 2$), the blocks of microfibrils (Fig. 10a, A and B) rotate while slipping between them (Fig. 10b), which is observed as lamellar rotation as a whole. For larger v_2, slipping is not limited between the blocks but it occurs also within each block, i.e., between microfibrils, with or without accompanying c-axis tilting within crystals. This local deformation gives rise to two types of microfibrils, probably depending upon the crystalline state of the film: (i) microfibril extending straight (Fig. 10c), and (ii) microfibril bending at the boundary between crystalline and amorphous parts (Fig. 10e). In the former case, the simple relation $L_p = L_0(\theta_w - \theta_s)$ holds as shown in the previous paper,[1] while in the latter case, L_p fails to obey this rule, which is the case of the present study.

When v_2 is close to 2 (range A), the deformation is so slight (in this example $\theta_w = \varphi$, as shown in Fig. 8) that it is understood without difficulty

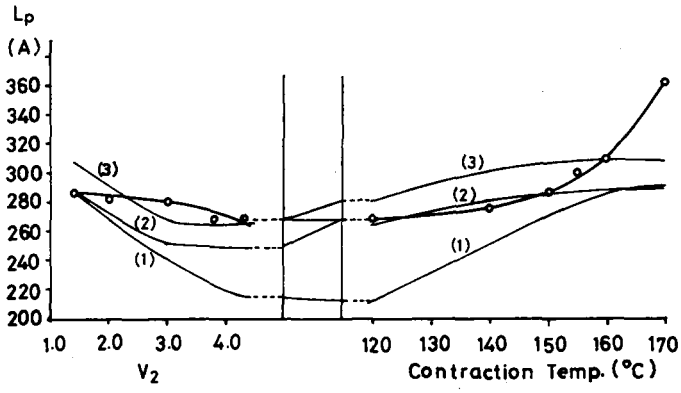

Fig. 11. Change in L_p during restretching at 152°C and subsequent thermal contraction: (O) observed L_p; (1) calculated with $L_p = 287 \cos(\theta_w - \theta_s)$; (2) calculated with $L_p = 287 \cos(\varphi - \theta_s)$; (3) calculated with $L_p = 306 \cos(\varphi - \theta_s)$.

that the orientation returns reversibly during the contraction (Fig. 10c, 10a). However, when v_2 is larger than 2, an indentation of the lamellar surface is developed by slipping between microfibrils (Fig. 10e), and orientation becomes more complex. The indentation also may possibly result from slipping between the extending microfibrils (Fig. 10d); however, the case (Fig. 10e) seems to be more probable from the observation that θ_w is larger than φ.

When the film contracts, the above-mentioned processes go backward, excepting the change in θ_s, which continues to increase further. However, this unexpected increase in θ_s does not necessarily mean the progressively increasing rotation of lamellae themselves; instead, it may be considered as the result of slipping backward between blocks of microfibrils so as to smooth the lamellar surface. It is noticeable here that θ_s is the angle between *pp* and the normal to the envelope of indented surface.

The sharp drop of θ_w above 155°C, while keeping φ and θ_s at 45°, seems to be due to recovery of tilting without largely displacing the microfibrils from the 45° position.

As to the long period of the restretched film, the observed L_p is considerably larger than that calculated from expression (1), as Figure 11 shows. This is attributable to the fact that the microfibril is bending at the boundary between crystalline and amorphous parts as mentioned above, where the expression should be modified as in (2), providing the microfibril bending is not so large that L_0 is used for calculation instead of *OD* (ref. Fig. 10e) because L_0 and *OD* are approximately equal to each other:

$$L_p = L_0 \cos(\varphi - \theta_s). \tag{2}$$

However, L_p calculated under this assumption is still smaller than the observed value in the case of the restretched film, while both values are in good agreement with each other in the case of the contracted film unless the temperature of contraction exceeds 150°C. When L_0 is assumed to be 306

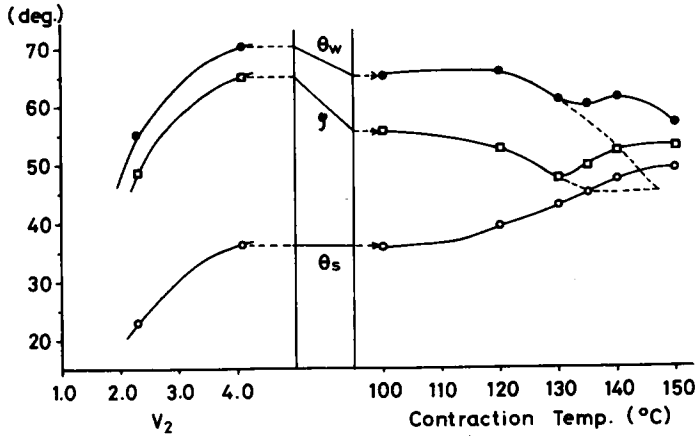

Fig. 12. Change in orientation parameters during restretching at 130°C and subsequent thermal contraction.

Å instead of the original value of 287 Å, the calculated and the observed values are in good agreement even for v_2 larger than 2. The value of 306 Å is not unreasonable when it is considered that the microfibrils sustain so large a stress during the high restretching and are frozen in that state. This elongation of L_0 (about 6–7%) is expected to recover when the film is heated to higher temperature; and, in fact, the observed value coincides well with the one calculated by using expression (2) with L_0 = 287 Å but not 306 Å for the contracted film.

Even these considerations are not sufficient to explain the extremely larger increase in long period of the film contracted above 150°C. This should be attributed to the annealing effect during the thermal contraction at the high temperature which has never been experienced by the film.

When a biaxial stretching [2-2FI](152)$_p\langle 2.7 \times v_2\rangle$ was carried out on the same film sample B_6 and subsequent contraction was performed from the states $v_1 \times v_2$ = 2.7 × 3.0 and 2.7 × 4.0, similar results are obtained as above. Therefore, a slight difference in v_1 or v_2 in such a degree seems to barely affect the basic deformation mechanism.

$$B_3,\ [2\text{-}2FI](130)_p\langle 2.8 \times v_2\rangle$$

In this experiment, sample B_3 of similar character was used, and the temperature of biaxial stretching was lowered to 130°C from 152°C ($T_1 = T_2$). The basic phenomenon was not affected by such difference in the experimental condition, excepting the final stage of contraction. The orientation parameters changed in this case not monotonously as seen in Figure 12, where it may be considered that the parameters change in two stages, as indicated by the broken line in the figure. The contraction behavior up to 130°C is principally similar to that observed in the preceding section. The first stage of contraction up to 135°C is two-dimensional, as

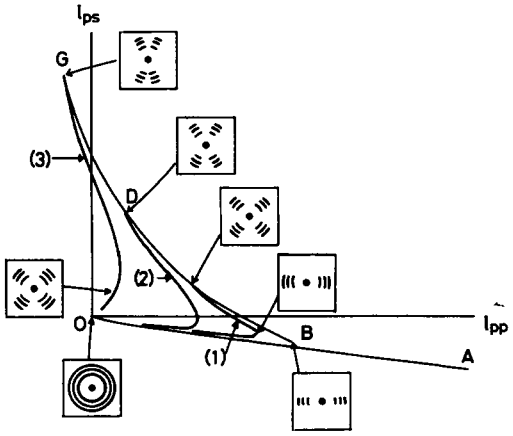

Fig. 13. Schematic diagram of WAXD pattern related to dimensional change during stretching, restretching, and thermal contraction.

observed in the 152°C stretching and the second stage above that temperature concerns the three-dimensional change. Therefore, the contraction in the latter stage is much more complex and it is not clear at the present time.

Later, however, the authors found that θ_w of a film prepared by [2-2FI] $(130)_p\langle 4 \times 4\rangle$ stretching decreased somewhat below 45° from the original value of 70° when the film was contracted at 170°C. Of course, the x-ray diagram in the final stage is of uniaxial orientation even though the arcs are considerably broadened. Therefore, whether θ_w remains not smaller than 45° (range B) or decreases below 45° (range A) seems to be determined not necessarily only by the ratio of v_1 to v_2.

This disorientation behavior is likely related intimately to the dimensional change during the thermal contraction. Figure 13 schematically represents thermal contraction behavior through dimensional change of the film as already illustrated in Figure 5. As partly reported in the previous paper,[2] a restretched film has a good memory of the stretching and restretching process the film suffered, and the film changes its dimension backward along the l_{pp}–l_{ps} curves shown during the restretching and stretching unless the biaxial orientation of the film exceeds the balanced state, while the film gradually loses the memory and the contraction curve gradually deviates from the above-mentioned behavior, as shown by the curves 2 and 3 in Figure 13 as the restretching has been performed more highly beyond the balanced state. The deviation of the l_{pp}–l_{ps} curve increases also with elevation of the restretching temperature. This temperature effect seems to be severe.

A part of the fine structure induced by stretching is destroyed by subsequent restretching but restructured in a new arrangement along the direction *ps*, accommodating the stress acting on the film. The accommodation of the new texture is more easy and the resulting texture is more stable when the restretching is carried out at higher temperature than when it is carried out at low temperature. Therefore, contraction and disorientation proceed

beyond the symmetrical biaxial orientation before the partial melting begins at about 155–160°C, and randomization is severe in the case of 130°C restretched film but not in the 152°C restretched film. This is the reason why range B can be distinguished from range A, but this demarcation is not absolute. Hence, the example supposedly lying between range A and range B is possible, though it is not frequently observed.

In summary, it is found that the contraction behavior of restretched film with type II orientation depends upon the degree of restretching. In the case of the film restretched not beyond the balanced state, the crystalline lamella returns to the state before restretching, i.e., the state of uniaxially stacked lamellae and does not randomize toward the three-dimensionally isotropic state until partial melting begins at about 155–160°C.

However, when the film has been restretched beyond the balanced state, the film contracts toward the symmetric biaxial orientation and, in the last stage of contraction, randomizes toward the three-dimensionally isotropic orientation, without passing the state of uniaxial lamellar stack.

Orientation and disorientation of the overbalanced film proceed two-dimensionally. This behavior corresponds well with the changes in film dimension and refractive index. The present discussion does not describe the effect of unfolding. However, there is no evidence of denying unfolding during the restretching, rather a small fraction of the weakest crystals is expected to be unfolded along with rotation of lamellae from the observation of incomplete irreversibility of restretching and contraction. As T_2 rises, this trend becomes more and more remarkable and type II orientation seems to convert gradually to Type III orientation as discussed in part VIII of this series of studies.[1] When the restretching is carried out to a much higher extent such as $v_2 > 7$–10, the contraction behavior is out of the mentioned scope because of the unfolding and development of fiber structure within the film.

The authors wish to thank Dr. Masahide Yazawa of the Polymer Processing Research Institute for financial support.

References

1. S. Okajima, N. Iwato, and H. Tanaka, *J. Polym. Sci. B*, **9**, 797 (1971).
2. H. Tanaka, K. Kurihara, M. Morita, K. Mori, and S. Okajima, *J. Polym. Sci. B*, **9**, 723 (1971).
3. S. Okajima and K. Homma, *J. Appl. Polym. Sci.*, **12**, 411 (1968).
4. H. Tanaka, T. Masuko, K. Homma, and S. Okajima, *J. Polym. Sci. A-1*, **7**, 1997 (1969).
5. T. Masuko, H. Tanaka, and S. Okajima, *J. Polym. Sci. A-2*, **8**, 1565 (1970).
6. H. Tanaka, T. Masuko, and S. Okajima, *J. Polym. Sci. A-1*, **7**, 3351 (1969).
7. H. Tanaka, T. Masuko, and S. Okajima, *J. Appl. Polym. Sci.*, **17**, 1715 (1973).
8. N. Iwato, H. Tanaka, and S. Okajima, *J. Appl. Polym. Sci.*, **17**, 2533 (1973).
9. S. Okajima, K. Kurihara, and K. Homma, *J. Appl. Polym. Sci.*, **11**, 1703 (1967).
10. F. J. Baltá-Calleja and A. Peterlin, *J. Macromol. Sci.-Phys.*, **B4**, 519 (1970).
11. J. B. Kinsinger and R. E. Hughes, *J. Phys. Chem.*, **63**, 2002 (1959).

Received May 17, 1974